Structural Analysis of the Progressive Die Bending Process for a High-Temperature Superconductor Stacked in Conduit Conductor

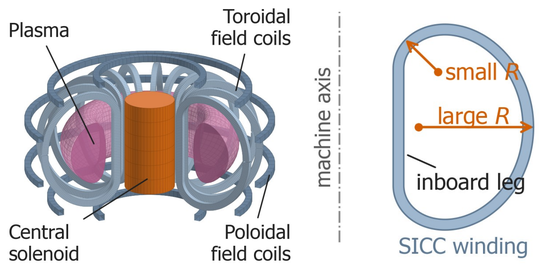
Jongseo Lee, Byungsu Lim, Kyung Mo Kim*

Department of Energy Engineering, Korea Institute of Energy Technology (KENTECH),
Kentech-gil 21, Naju-si, Jeollanam-do 58330, Republic of Korea
ibanabbb314@kentech.ac.kr, bslim@kentech.ac.kr, kmokim@kentech.ac.kr

KENTECH Korea Institute of Energy Technology

한국원자력학회 Korean Nuclear Society

1. Introduction



$$\varepsilon(y) = \varepsilon_0 + \kappa y$$

y from the stack centre, $\kappa = 1/R$ curvature, ε_0 uniform part (0 in pure bending)

$$\varepsilon_{\text{tape}} = \varepsilon_0 + \kappa c \le \varepsilon_{\text{allow}} = 0.30\,\%$$

at the outermost tape $y = c$, below the 77 K critical-current (I_c) limits of 0.28–0.72 % [1]–[3]

Fig. 1. Schematics of (a) a tokamak magnet system and (b) a D-shaped toroidal field (TF) coil

- The TF coil (Fig. 1) of the Korean compact fusion device **K-CPD** uses a REBCO **stacked in conduit conductor (SICC)** of non-transposed tapes, a cap, a Cu double helix and a jacket [4], [5], formed by **progressive die bending**.
- The target is the beam-theory radius for $\varepsilon_{\text{allow}}$, $\boldsymbol{R_t = 1.256}$ **m**. The tape strain inside the jacket **cannot be measured during forming** and is analysed here ahead of the prototype bending test.

Objective This study investigates both the adherence of tape strain to the allowable limit ($\varepsilon_{\text{allow}}$) at R_t and the degree to which die-induced bending is transmitted to the tape.

2. Conductor and Bending Process

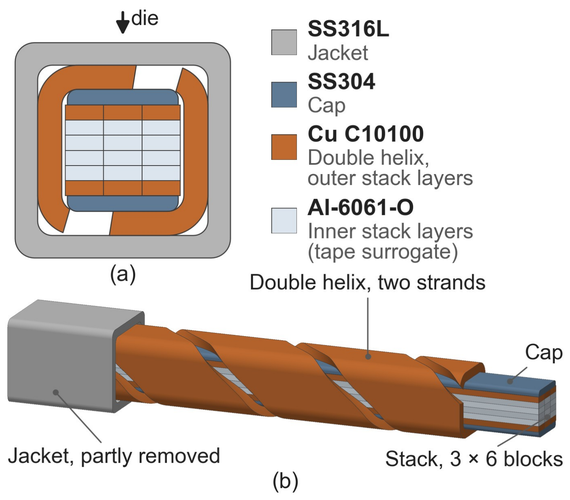


Fig. 2. Finite element (FE) model, (a) section beneath the centre die and (b) cutaway view

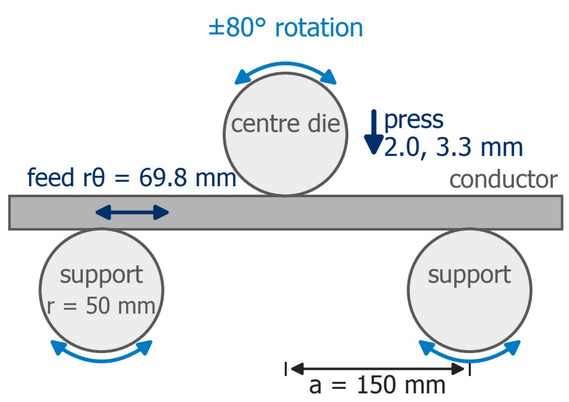


Table I. HTS stack, c from the stack centre

Quantity	Value
Layers through the stack	6
Outer layer on each side	Cu, no tape
Stack height	11.30 mm
Outermost tape layer, c	3.767 mm

Target radius. With no coil radius specified, pure bending ($\varepsilon_0 = 0$) with $\kappa c = \varepsilon_{\text{allow}}$ gives

$$R_t = \frac{c}{\varepsilon_{\text{allow}}} = 1.256\ \text{m}$$

and the target curvature $\boldsymbol{\kappa_t = 1/R_t = 0.796\ m^{-1}}$.

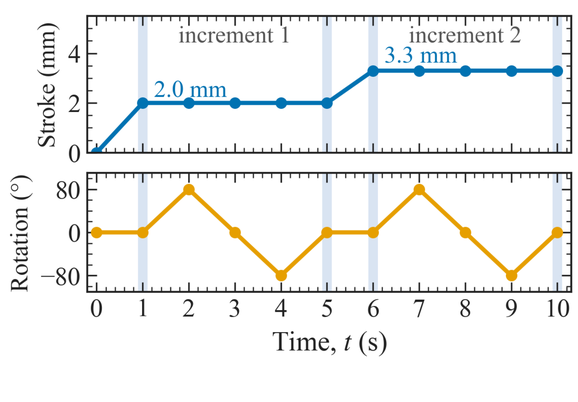


Fig. 3. (a) Three-die bending and (b) stroke and rotation, 1 s press and 4 s rotation per increment

- The conductor (Fig. 2, Table I) is bent in **increments** of a **1 s press** and **four 80° rotations** of the dies, which roll it by 69.8 mm and back (Fig. 3).
- The second press of **3.3 mm** was interpolated to κ_t from the die-centre curvature after the rotations of an earlier 2 mm-step schedule.

3. FE Model and Strain Evaluation

Table II. Material models with multilinear isotropic hardening

Component	Material	E (GPa)	Initial yield (MPa)
Jacket	SS316L	193	300
Cap	SS304	193	510
Double helix, outer stack layers	Cu C10100	117	69
Inner stack layers (tape surrogate)	Al-6061-O	68.9	55

- Static large-deflection analysis in ANSYS Mechanical 2025 R2 (244,759 elements), with frictional die contacts ($\mu = 0.25$) and bonded internal interfaces.
- The tape region is an **Al-6061-O surrogate** (Table II) that yields at 0.08 %.

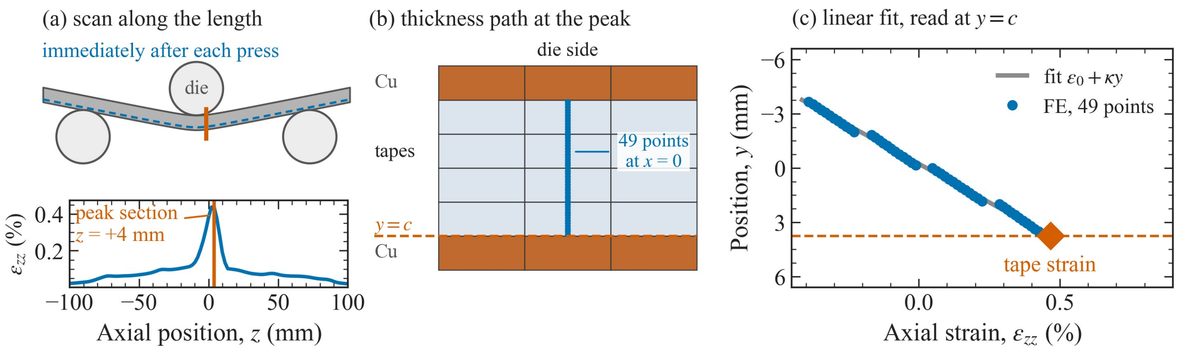


Fig. 4. Evaluation of the tape strain, shown for the 3.3 mm press (sketch in (a) not to scale)

- The axial strain is scanned along the conductor to locate the **peak section**, where the fit $\varepsilon_0 + \kappa y$ through the thickness gives the **tape strain** at $y = c$, immediately after each press (Fig. 4). The proceedings used the stack maximum.

4. Results and Discussion

4.1 Stress and strain concentrate beneath the centre die

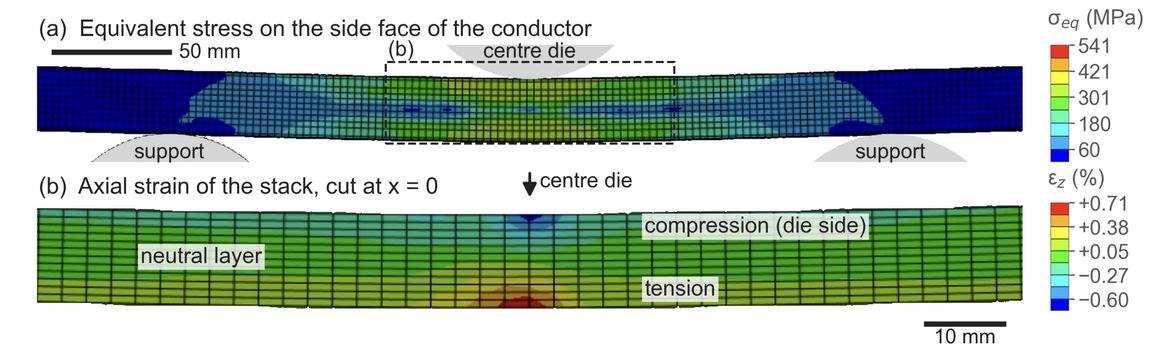


Fig. 5. FE fields after the 3.3 mm press ($t = 6$ s, true scale, die side up)

- Beneath the die the jacket exceeds its 300 MPa yield stress (Fig. 5).

4.2 The bend localizes beneath the centre die

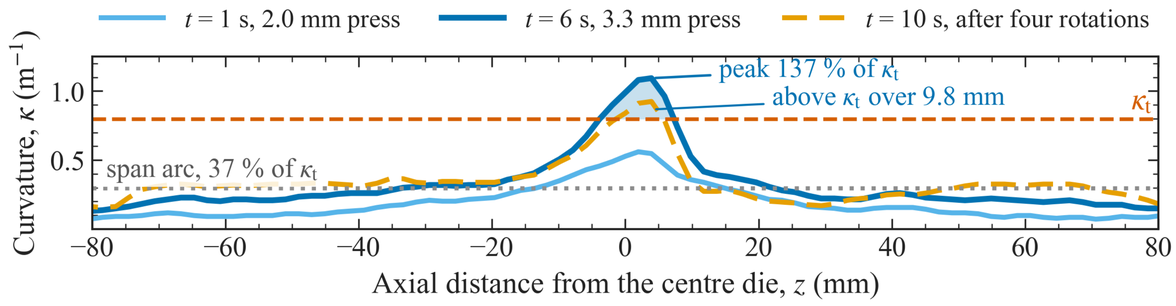


Fig. 6. Local curvature along the conductor, obtained from the deflection of the stack

- After the 3.3 mm press the peak reaches **137–147 % of κ_t** (two methods, Fig. 6) against **37 %** for the span arc, and κ_t is exceeded over only **9.8 mm**.
- The tapes follow this local curvature, with ε_0 of only 0.027 % (Fig. 4).
- During the rotations the conductor bends 40–80 mm away (+36–49 %), the force decreases to 3.6 kN, and the peak recovers elastically (tape strain −15 %).

4.3 A plastic hinge sets the stroke

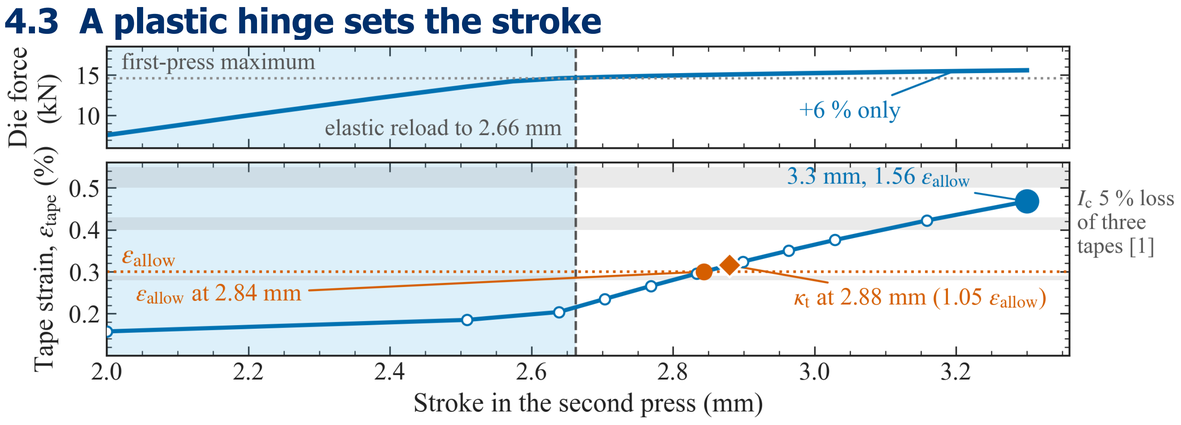


Fig. 7. Die force and peak-section tape strain in the second press, from solver sub-steps (each equal to a press stopped at that stroke)

- Beyond the elastic reload to **2.66 mm** (Fig. 7), a further **6 %** in die force raises the tape strain from 0.22 to 0.47 %, the signature of a **plastic hinge**.
- $\varepsilon_{\text{allow}}$ is reached at **2.84 mm** (local R = 1.32 m) and κ_t at **2.88 mm** with **1.05 $\boldsymbol{\varepsilon_{\text{allow}}}$**, the excess over κc being ε_0. Each 0.1 mm adds about 0.04 %.
- The present 3.3 mm press gives **0.468 % (1.56 $\boldsymbol{\varepsilon_{\text{allow}}}$)**.

5. Conclusion

(i) **Allowable strain.** At a local radius of R_t the tape strain is already 1.05 $\varepsilon_{\text{allow}}$ because of ε_0, and the present 3.3 mm press **exceeds $\boldsymbol{\varepsilon_{\text{allow}}}$** (1.56 $\varepsilon_{\text{allow}}$, above two of the three tapes in [1]). **$\boldsymbol{I_c}$ degradation is expected.**

(ii) **Bend transfer.** The excess is confined beneath the centre die, where the die bend concentrates in a **plastic hinge** (3.7–4.0 times the span-arc curvature, above κ_t over only 9.8 mm), and the tapes follow this local curvature.

(iii) **Bending procedure.** The stroke should be limited by the **tape strain at the peak section immediately after the press**, not by the die-centre curvature after rotations. Beyond the 2.66 mm elastic reload each 0.1 mm adds about 0.04 %, limiting the second press to **2.84 mm**. As the span arc is only 37 % of κ_t at 3.3 mm, R_t is expected to require **smaller, repeated presses with feeding** to spread the bend (under analysis), as the rotations already bend it 40–80 mm away.

(iv) **Limitations.** The results are for the loaded state at one die position, bonded internal interfaces, an Al tape surrogate and 77 K strain limits applied to room-temperature forming. Actual tape properties, interface slip, unloading, the helix pitch and the prototype bending test remain to be examined.

References

[1] R. He et al., Bending and Uniaxial Tensile Strain Effects on the Critical Current of REBCO Coated Conductor Tapes, Cryogenics, Vol. 116, 103285, 2021.
[2] C. Barth, G. Mondonico, and C. Senatore, Electro-mechanical Properties of REBCO Coated Conductors from Various Industrial Manufacturers at 77 K, Self-field and 4.2 K, 19 T, Supercond. Sci. Technol., Vol. 28, 045011, 2015.
[3] C. Zhou et al., Critical Current of Various REBCO Tapes Under Uniaxial Strain, IEEE Trans. Appl. Supercond., Vol. 26, No. 4, 8401304, 2016.
[4] S. Oh et al., Preliminary Design Study on Non-Twisted HTS Conductor for Fusion Applications, IEEE Trans. Appl. Supercond., Vol. 33, No. 5, 4801505, 2023.
[5] K. M. Kim, J. S. Lee, and B. S. Lim, Structural Analysis of High-Temperature Superconductor Winding Based on Stacked in Conduit Conductor Design, EUCAS, 1-MP-PM.198, 2025.